学位論文

Differential effects of depot formulations of GnRH agonist leuprorelin and antagonist degarelix on the seminiferous epithelium of the rat testis

(GnRH agonist の leuprorelin と antagonist の degarelix がラット曲精細管上皮の微細構造に及ぼす影響の比較)

旭川医科大学大学院医学系研究科博士課程医学専攻

堀　淳一

(甲賀　大輔、柿崎　秀宏、渡部　剛)

Biomedical Research (Tokyo) **39** (4) 197–214, 2018

Differential effects of depot formulations of GnRH agonist leuprorelin and antagonist degarelix on the seminiferous epithelium of the rat testis

Jun-ichi Hori[1, 2], Daisuke Koga[1], Hidehiro Kakizaki[2], and Tsuyoshi Watanabe[1]
[1] Department of Microscopic Anatomy and Cell Biology, and [2] Department of Renal and Urologic Surgery, Asahikawa Medical University, Asahikawa, Japan

(Received 16 May 2018; and accepted 2 June 2018)

ABSTRACT

Despite their pharmacologically opposite actions, long-acting depot formulations of both GnRH agonists and antagonists have been clinically applied for treatment of androgen-sensitive prostate cancer. Sustained treatment with GnRH analogues commonly suppresses both the synthesis and release of gonadotropins, leading to depletion of testicular testosterone. To clarify the underlying differences in the effects of GnRH agonists and antagonists on spermatogenesis, we compared histological changes in the seminiferous epithelium after administration of depot formulations of GnRH agonist leuprorelin and antagonist degarelix to male rats. Testicular weight had markedly declined by 28 days after administration of both GnRH analogues, although the testicular weight was decreased more promptly by leuprorelin compared with degarelix. Shortly after administration, massive exfoliation of premature spermatids and anomalous multinucleated giant cells was observed in seminiferous tubules of leuprorelin-treated rats, probably via the initial hyperstimulatory effects on the hypothalamic-pituitary-testicular axis, whereas no discernible changes were found in those of degarelix-treated rats. Long term treatment with both types of GnRH analogues similarly induced a marked reduction in the height of the epithelium and deformation of apical cytoplasm in Sertoli cells, resulting in premature detachment of spermatids from the epithelium. Lipid droplets had accumulated progressively in Sertoli cells, especially in those of degarelix-treated rats. These findings clearly demonstrate the differences in the effects of GnRH agonists and antagonists on the spermatogenic process. This study suggests that an appropriate choice of GnRH analogues is necessary to minimize their adverse effects on spermatogenesis when reproductive functions should be preserved in patients.

Male gametes of mammals, spermatozoa, are generated from spermatogonial stem cells in a stepwise fashion by mitosis and meiosis in the seminiferous tubules of testes (16, 22). The stem and developing spermatogenic cells, including spermatogonia, spermatocytes, spermatids, and spermatozoa, are supported both structurally and metabolically by surrounding Sertoli cells in the seminiferous epithelium (15, 44) where spermatogenesis, a series of differentiation processes of spermatogenic cells to mature spermatozoa, occurs. At the basal compartment of the seminiferous epithelium below the blood-testicular barrier (BTB) formed by adjacent Sertoli cells, spermatogonia proliferate and differentiate into spermatocytes. The generated preleptotene spermatocytes are then translocated to the adluminal compartment above the BTB, where meiosis is completed and successive spermiogenesis from round premature spermatids to elongated mature spermatids proceeds (41, 64).

Spermatogenesis in mammalian seminiferous tubules is elaborately regulated by the hypothalamic-

Address correspondence to: Dr. Tsuyoshi Watanabe, Department of Microscopic Anatomy and Cell Biology, Asahikawa Medical University, Midorigaoka-higashi 2-1-1-1, Asahikawa 078-8510, Japan
Tel: +81-166-68-2310
E-mail: tyshwata@asahikawa-med.ac.jp

pituitary-testicular axis (37). Gonadotropin-releasing hormone (GnRH) discharged from hypothalamic neurons into the hypophyseal portal system acts on gonadotropes in the anterior pituitary gland to secrete two gonadotropins, luteinizing hormone (LH) and follicle-stimulating hormone (FSH), into systemic circulation (5). In male mammals, both gonadotropins act on the testes to facilitate reproductive functions. FSH acts directly on Sertoli cells in seminiferous tubules, while LH facilitates testosterone production in Leydig cells located among seminiferous tubules. In turn, testosterone secreted from Leydig cells acts on Sertoli cells to facilitate and maintain spermatogenesis in collaboration with FSH (3, 45, 59).

GnRH analogues generated by substitution of amino acid residues of intrinsic GnRH bind competitively to the GnRH receptor on pituitary gonadotropes, resulting in augmentation (by agonists) or attenuation (by antagonists) of intracellular signaling events downstream of the receptor (11, 24, 29). However, long term treatment with powerful GnRH agonists such as buserelin (7) and leuprorelin (36), paradoxically suppresses both synthesis and secretion of gonadotropins by receptor desensitization, which contrasts their original and initial stimulatory effects on gonadotropes (23). In contrast to the agonists, depot formulations of GnRH antagonists, such as degarelix (8), intensely suppress the secretion of pituitary gonadotropins upon administration (46). In any case, continuous administration of GnRH analogues effectively suppresses synthesis and secretion of pituitary gonadotropins in the chronic phase, resulting in depletion of serum androgens/estrogens derived from gonads. Thus, long-acting depot formulations of GnRH agonists and antagonists have been widely applied for treatment of sex steroid-dependent diseases such as endometriosis, uterine leiomyoma, prepubertal maturation, and metastatic prostate cancer (1, 11, 14, 39).

Although previous studies have largely clarified the molecular mechanisms underlying the inhibitory effects on pituitary gonadotropes after administration of long-acting GnRH analogues as described above, the differences in the effects of these two opposing types of GnRH analogues, agonists and antagonists, on the testes located downstream of the pituitary have not been sufficiently investigated so far. In the present study, we compared histological and cytological changes in seminiferous tubules of the rat testis after administration of depot formulations of GnRH agonist leuprorelin and antagonist degarelix. Morphological changes in the seminiferous epithelium of acute and chronic phases after administration of the depot formulations of the two types of GnRH analogues clearly indicated both differences and similarities in their effects on spermatogenesis. Based on the distinct temporal courses of the histological changes in the seminiferous epithelium after administration of the depot formulations of the GnRH agonist and antagonist, we discuss the profound differences in the mechanisms of these two types of GnRH analogues, leading to suppression of spermatogenesis in the seminiferous epithelium.

MATERIALS AND METHODS

Animals and experimental procedures. One hundred and thirty two adult male Wistar rats (body weight: ca. 200 g) were divided into 11 experimental groups (12 rats each) and kept in plastic cages placed in a well-ventilated room (23–25°C; 55–65% relative humidity) with food and water provided *ad libitum*. To evaluate changes in the plasma LH concentration in the early phase of treatments (4 h, 8 h, and 2 days after the onset of treatment), additional 24 adult male rats were divided into six experimental groups (four rats each) and kept under the same conditions described above.

At 8 weeks of age, the rats of the eight groups (five groups with 12 rats each, and three groups with four rats each) were subcutaneously injected with 1.5 mg/kg GnRH agonist depot [leuprorelin (leuprolide acetate) for one-month depot suspension (3.75 mg/mL); Takeda Pharmaceutical Co., Osaka, Japan], while the rats of another eight groups (five groups with 12 rats each, and three groups with four rats each) at 8 weeks of age were subcutaneously injected with 2 mg/kg GnRH antagonist depot [degarelix (degarelix acetate) for one-month depot suspension (20 mg/mL); Astellas Pharma Inc., Tokyo, Japan]. These one-month depot formulations can continuously release an effective dose of GnRH analogues over one month after administration by single injection (8, 34). These rats were maintained for various durations (4 h to 28 days) and then used for experiments as described below. The rats of one group (12 rats) received only the suspension vehicle and were used directly for experiments as controls.

The rats were used for experiments in accordance with the Guide for the Care and Use of Laboratory Animals (Institute of Laboratory Animal Resources, National Research Council, Washington, DC, 1996) under permission of the Experimental Animal Welfare Committee of Asahikawa Medical University (permission # 16032).

Measurement of plasma LH. After rats were anesthetized with ketamine/xylazine (100 : 10 mg/kg body weight), blood was collected into tubes containing heparin (100 U per tube) by puncture of the inferior vena cava ($n = 4$ per experimental group). The blood samples were then centrifuged at 4°C for 10 min, and the plasma of each sample was divided into aliquots and stored at −20°C until analysis. Testes were also excised from each rat and processed for histological analysis as described below after their wet weight was measured to evaluate the effects of GnRH agonist and antagonist depots.

Plasma concentrations of LH were measured using a commercially available enzyme-linked immunosorbent assay (ELISA) kit (rodent LH ELISA test kit, product code: ERKR7010; Endocrine Technologies Inc., Newark, CA, USA), according to the manufacturer's instructions. The amounts of LH in samples were calculated by a corresponding standard curve and expressed as ng of the standard preparation of rat LH provided by the supplier. Statistical analyses were performed as described below.

Histological and morphometrical analyses. For histological assessment of the effects of GnRH analogues, the testes excised from rats after sampling blood plasma were fixed in Bouin's solution, rinsed in 0.1 M phosphate buffer (PB; pH 7.4), dehydrated in a graded ethanol series, and embedded in paraffin. Sections (8 μm thick) cut from the paraffin-embedded tissue blocks were stained with hematoxylin and eosin.

Five independent fields in a hematoxylin and eosin-stained section per rat (20 fields in four independent rats per experimental group) were selected with sufficient spacing to avoid double sampling and photographed under a light microscope equipped with a ×10 objective lens (Olympus, Tokyo, Japan).

The individual profile diameters of seminiferous tubules in each photograph were measured with ImageJ software (National Institutes of Health, Bethesda, MD, USA; https://imagej.nih.gov/ij/). The means and related statistical parameters of the diameters were calculated and analyzed with KaleidaGraph software (Synergy Software, Reading, PA, USA).

To evaluate the occurrence of multinucleated giant cells in seminiferous tubules, the numbers of both the cross-sectioned profiles of seminiferous tubules containing multinucleated giant cells and those containing no multinucleated giant cells were counted in each photograph, and then the numbers of those containing multinucleated giant cells were divided by the corresponding total number of the cross-sectioned profiles of seminiferous tubules in each experimental group. Temporal changes in the fraction of the profiles of seminiferous tubules containing multinucleated giant cells were compared between experimental groups treated with GnRH agonist leuprorelin and antagonist degarelix. All morphometrical parameters obtained were statistically analyzed as described below.

Scanning electron microscopy of KOH-digested tissues. The three-dimensional (3D) ultrastructure of rat seminiferous tubules in each experimental group was analyzed by scanning electron microscopy (SEM) after preparation of testicular tissues according to the simple KOH digestion method by Ushiki and Ide (55). Briefly, rats ($n = 2$ per experimental group) anesthetized with ketamine/xylazine were perfused with 30 mL physiological saline and then with 100 mL of 2% glutaraldehyde (GA) in 0.1 M PB, pH 7.4. The testes were quickly excised, cut into small pieces, and immersed in the same fixative at 4°C for 24 h. After rinsing the fixed tissues several times in 0.1 M PB (pH 7.4), the tissues were placed in 30% KOH for 8–10 min at 60°C. The tissues digested with KOH were washed thoroughly in 0.1 M PB (pH 7.4) and then treated with 1% tannic acid (Nacalai Tesque, Kyoto, Japan) in 0.1 M PB for 1 h, rinsed in the buffer for 1 h, and immersed in 1% osmium tetroxide (OsO_4) as a conductive stain for 1 h. The samples were then dehydrated through a graded ethanol series, transferred to isoamyl acetate, and dried in a critical point dryer (model HCP-2; Hitachi Koki Co. Ltd, Tokyo, Japan). Dried specimens were then mounted on aluminum stubs with silver paste, coated with platinum-palladium in an ion-sputter coater (model E1010; Hitachi Koki Co. Ltd) and observed under a scanning electron microscope (model S-4100; Hitachi High Technologies, Tokyo, Japan).

Correlative light microscopy and SEM of Epon-embedded semithin sections. Epon-embedded semithin sections of the testis were correlatively observed by both light microscopy and BSE-mode SEM, as described previously (20). Briefly, rats ($n = 3$ per experimental group) anesthetized with ketamine/xylazine were perfused with 30 mL physiological saline and then with 100 mL of 2% GA/2% paraformaldehyde (PFA) in 0.1 M PB, pH 7.4. The testes were quickly excised, cut into small pieces, and immersed in the same fixative at 4°C for 24 h. After washing thoroughly with 0.1 M PB containing 7.5% sucrose (pH 7.4), the samples were postfixed with 1% OsO_4

in 0.1 M PB containing 7.5% sucrose at 4°C for 2 h. After postfixation, the samples were dehydrated using a graded ethanol series and embedded in Epon 812. Semithin sections of tissues embedded in Epon 812 resin prepared with an ultramicrotome (model EM UC7; Leica, Wetzlar, Germany) were carefully picked up with a 7-mm diameter aluminum loop (Transfer ring; Micro Star Co., Tokyo, Japan) and mounted on a glass slide by heating on a hot plate at 50°C for 30 min. After the semithin sections were stained with toluidine blue, they were first viewed and photographed under the light microscope equipped with the ×10 objective lens. The semithin sections were then counterstained with uranyl acetate and lead citrate for electron microscopy. After the semithin sections were coated with OsO_4 at a thickness of 1 nm using an osmium coater (model HPC-20; Vacuum Device, Ibaraki, Japan), the sections were viewed under a cold field emission-type scanning electron microscope equipped with a highly sensitive semi-annular semiconductor BSE detector (model SU-8240; Hitachi High Technologies). The corresponding regions of interest in the semithin sections were imaged using the BSE detector at an accelerating voltage of 2 kV.

Antisera. Rabbit polyclonal anti-espin (product code: NBP1-90588) and mouse monoclonal anti-zonula occludens-1 (ZO-1; product code: 33-9100) antibodies were purchased from Novus Biologicals (Littleton, CO, USA) and Thermo Fisher Scientific (Waltham, MA, USA), respectively. Secondary antibodies, Alexa Fluor 488-labeled donkey anti-rabbit IgG (product code: A-21206) and Alexa Fluor 594-labeled donkey anti-mouse IgG (product code: A-21203), were purchased from Thermo Fisher Scientific.

Immunofluorescence microscopy. Three rats from each experimental group anesthetized with ketamine/xylazine were perfused with physiological saline, followed by a solution of 4% PFA in 0.1 M PB containing 4% sucrose (pH 7.4). After fixation by perfusion, testes were immersed in the same fixative for 2 h at 4°C. After washing the fixed tissues thoroughly with 0.1 M PB containing 7.5% sucrose (pH 7.4), the tissues were immersed sequentially in 15% sucrose (6 h) and 30% sucrose (12 h) solutions buffered in 0.1 M PB (pH 7.4) at 4°C. Then, the tissue blocks were frozen in Tissue-Tek O.C.T. compound (Sakura Finetek, Tokyo, Japan) at −30°C. Tissue sections of 12 μm in thickness were cut from the frozen tissue blocks with a cryostat (model CM3050S; Leica Microsystems GmbH, Wetzlar, Germany) and mounted on microscope slides.

For immunocytochemical staining, tissue sections of the testis were treated with a 0.05% citraconic anhydride solution (Immunosaver; Nissin EM Co. Ltd., Tokyo, Japan) for 30 min at 60°C for antigen retrieval (28) and then incubated with 2% normal donkey serum (30 min, 20°C) for blocking. After these pretreatments, the tissue sections were incubated with a mixture of primary antibodies of different species (rabbit and mouse) for 16 h at 20°C. The sections were subsequently incubated with a mixture of appropriate sets of Alexa Fluor 488- and 594-labeled secondary antibodies for 1 h at 20°C. Between each step, the sections were washed three times in 0.01 M PB (pH 7.4) containing 0.5 M NaCl and 0.1% Tween 20. After a section was rinsed with PBS (3 min, three times), a coverslip was mounted on the tissue section in 90% glycerol (v/v in PBS) containing 0.1% p-phenylenediamine dihydrochloride (Sigma-Aldrich, St. Louis, MO, USA) and 4′,6-diamidino-2-phenylindole (DAPI; Sigma-Aldrich). The immunostained sections were viewed under a laser scanning confocal microscope (model FV-1000D; Olympus).

Statistical analysis. The results of ELISAs and morphometrical analyses were statistically analyzed with KaleidaGraph software by one-way analysis of variance (ANOVA), followed by the Tukey HSD post-hoc test when a significant interaction ($P < 0.05$) was calculated.

RESULTS

Changes in plasma hormone levels and testicular weights after administration of depot formulations of GnRH analogues

To evaluate the systemic effects of GnRH analogues on the hypothalamic-pituitary-testicular axis, we first measured the plasma LH concentration and wet weight of a testis at various time points after administration of depot formulations of GnRH agonist leuprorelin or antagonist degarelix to male rats.

The mean concentration of LH in the blood plasma of control male rats was 0.61 ± 0.15 ng/mL (mean ± SEM), just above the detection limit (0.5 ng/mL) of the LH-ELISA kit. The concentration of LH in blood plasma was markedly but transiently increased during the first 24 hours after administration of the depot formulation of leuprorelin and then rapidly decreased to the basal level by day 2 of the treatment. The low level of plasma LH was maintained until day 28 of treatment (Fig. 1A; solid line). Plas-

ma LH levels in rats receiving the depot formulation of degarelix were decreased below the detection limit immediately after the onset of treatment and never elevated above the detection limit throughout the experimental period (Fig. 1A; dotted line). These temporal changes in plasma LH levels confirmed that the difference in the effects between the GnRH agonist and antagonist on the secretion of pituitary gonadotropin(s) was consistent with those in previous reports (8, 19, 46).

Although the immunoreactive plasma LH measured with the ELISA kit was not decreased below the detection limit even after the acute hyperstimulated phase induced by the leuprorelin depot, the testicular weight was significantly decreased in response to leuprorelin administration. The wet weight of a testis from rats receiving the leuprorelin depot was decreased to about two-thirds, half, and one-third of those in control rats by 4, 7, and 14 days after the onset of treatment, respectively (Fig. 1B; solid line). The wet weight of a testis from rats receiving the depot formulation of degarelix was also reduced, but the temporal course of reduction was quite different from that of rats that received the leuprorelin depot. The weight of a testis decreased slowly during the first week after the onset of treatment, but was drastically reduced to approximately one-fourth of the control testis by day 14 of treatment. The reduction in testicular mass continued until day 28 of treatment (Fig. 1B; dotted line). These findings indicated that both GnRH agonist and antagonist depots suppressed the functional states of the hypothalamic-pituitary-testicular axis in the chronic phase, although the temporal patterns of the effects exerted by each GnRH analogue appeared to be different.

Histological changes in seminiferous tubules after administration of depot formulations of GnRH analogues

Because the temporal course of changes in the testicular weight of rats after receiving the leuprorelin depot was apparently different from that of rats receiving the degarelix depot, we next examined histological changes in the testis of each experimental group.

As seen in the micrographs of the hematoxylin and eosin-stained tissue sections of the testis, the diameter of seminiferous tubules in the testis of rats continuously treated with GnRH analogues was apparently reduced in the chronic phase from day 14 to 28 of treatment (Fig. 2). This result indicated that both leuprorelin and degarelix depots induced atro-

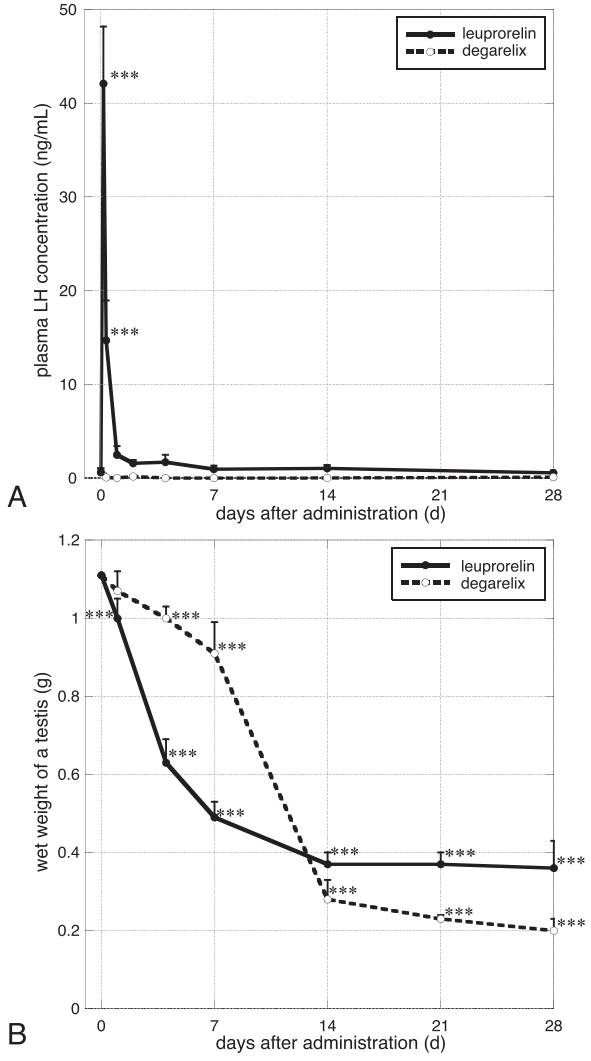

Fig. 1 Changes in the plasma LH concentration (A) and wet weight of the testis (B) after administration of depot formulations of GnRH agonist leuprorelin (solid lines) and antagonist degarelix (dotted lines). (**A**) Circles and error bars at each time point indicate the mean and SEM of the plasma LH concentration (ng/mL), respectively ($n = 4$ per experimental group). Temporal changes in the plasma LH concentration of each series of experimental groups, leuprorelin-treated (solid line) and degarelix-treated (dotted line) rats, were statistically significant by one-way ANOVA ($P < 0.001$ for both experimental groups). The values indicated by asterisks are significantly different compared with the control group (***$P < 0.001$; determined by Tukey HSD post-hoc test following one-way ANOVA). (**B**) Circles and error bars at each time point indicate the mean and SEM of the wet weight of a testis (g), respectively ($n = 4$ per experimental group). Temporal changes in the testicular weight of each series of experimental groups treated with GnRH agonist leuprorelin (solid line) and antagonist degarelix (dotted line) were statistically significant by one-way ANOVA ($P < 0.001$ for both experimental groups). The values indicated by asterisks are significantly different compared with the control group (***$P < 0.001$; determined by Tukey HSD post-hoc test following one-way ANOVA).

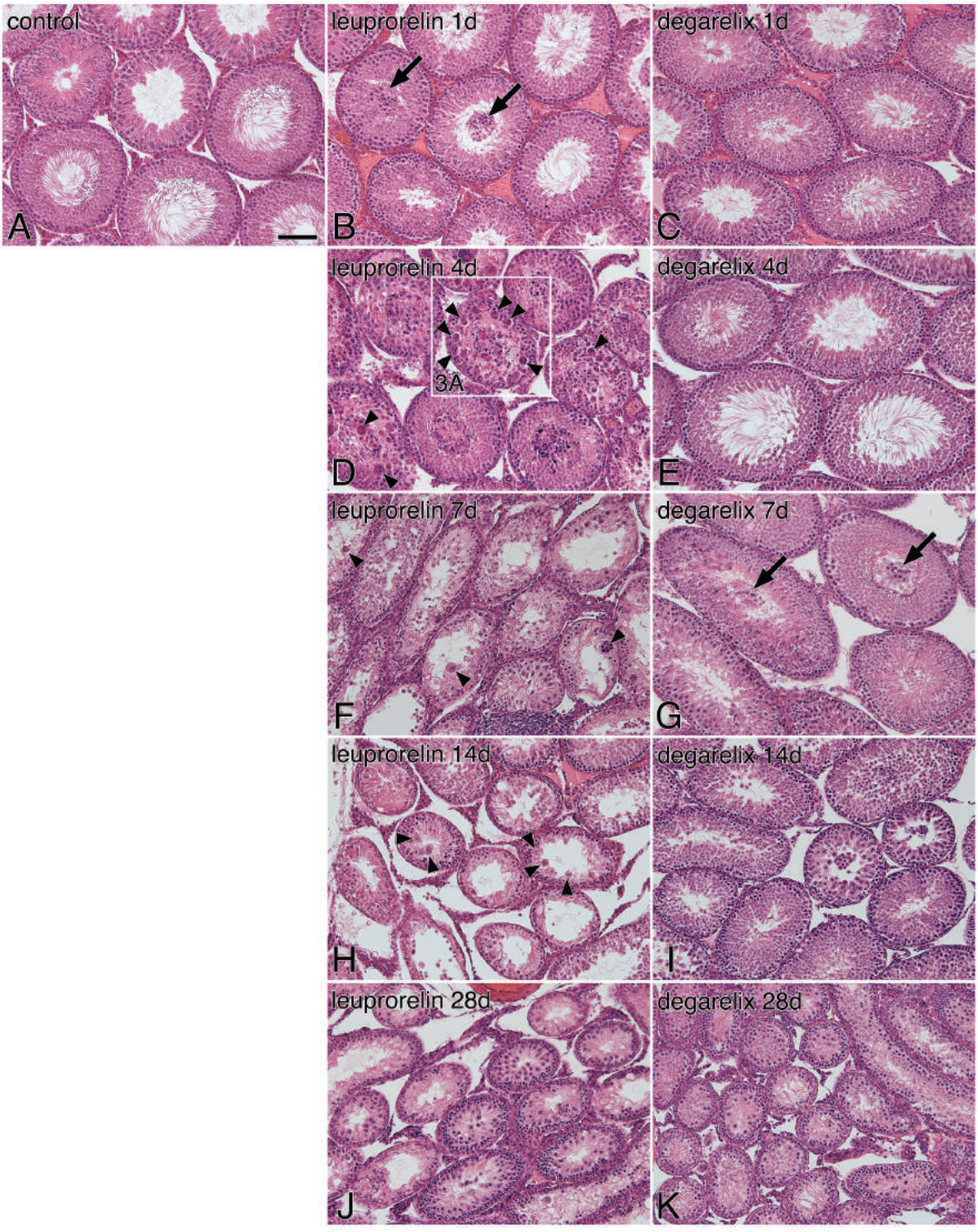

Fig. 2 Histological changes in seminiferous tubules after administration of depot formulations of GnRH agonist leuprorelin (B, D, F, H, J) and antagonist degarelix (C, E, G, I, K). Seminiferous tubules observed in the testis of a control rat are shown in (A). Each panel is a photograph at an identical magnification (Bar = 100 μm). The diameter of seminiferous tubules was apparently reduced in the chronic phase in both leuprorelin (H, J)- and degarelix (I, K)-treated rats compared with control rats (A). Note that massive exfoliation of premature spermatids (arrows) occurred in both leuprorelin- and degarelix-treated rats, but more promptly after administration in leuprorelin-treated rats (B) than in degarelix-treated rats (G). Note that multinucleated giant cells appeared specifically in the seminiferous tubules of leuprorelin-treated rats (D–F; arrowheads). The boxed area indicated with the white line in (D) is enlarged and shown in Fig. 3A.

Table 1 *Profile diameters of seminiferous tubules in the testis (left column) and occurrence of multinucleated giant cells in seminiferous tubules (right column)*

Experimental group		Diameter of seminiferous tubules (μm)	Occurrence of seminiferous tubules containing multinucleated giant cells (giant cell positive/total)
Control rats		260.4 ± 3.0	0.0% (0/96)
Leuprorelin-treated rats			
	Day 1	244.8 ± 1.9***	5.8% (6/103)
	Day 4	198.7 ± 2.6***	24.7% (44/178)
	Day 7	146.1 ± 1.7***	21.2% (42/198)
	Day 14	154.3 ± 1.6***	8.4% (16/190)
	Day 28	137.9 ± 1.6***	1.6% (4/247)
Degarelix-treated rats			
	Day 1	219.5 ± 2.9***	0.0% (0/116)
	Day 4	234.2 ± 2.6***	0.8% (1/121)
	Day 7	228.0 ± 3.5***	0.0% (0/114)
	Day 14	190.3 ± 2.0***	1.1% (2/179)
	Day 28	96.0 ± 1.0***	0.3% (1/388)

Each value is expressed as the mean ± S.E.M. To estimate the diameters of seminiferous tubules, 20 micrographs per experimental group were used. Statistically significant differences in the profile diameters of seminiferous tubules among the time points of each experimental group were detected by one-way ANOVA ($P < 0.001$ for both leuprorelin- and degarelix-treated groups). The values indicated by asterisks are significantly different compared with the control group (***$P < 0.001$; determined by Tukey HSD post-hoc test following one-way ANOVA). The percentages of profiles of seminiferous tubules containing multinucleated giant cells to the total number of profiles are shown in the right column. The numbers of profiles of seminiferous tubules observed for each experimental group are shown in parentheses.

phic changes in the testis. The mean diameter of seminiferous tubules in the testis of rats receiving the leuprorelin depot (Fig. 2B, D, F, H, J) was more rapidly reduced than that of rats receiving the degarelix depot (Fig. 2C, E, G, I, K; see also Table 1). In the lumen of seminiferous tubules of rats on 1 day after receiving the leuprorelin depot, large clusters of spermatogenic cells were abnormally liberated from the epithelial wall of seminiferous tubules (Fig. 2B, arrows). In addition, anomalous giant cells were frequently observed in the seminiferous epithelium of rats receiving the leuprorelin depot from day 4 to 14 of treatment (Fig. 2D, F, H, arrowheads). At a higher magnification, typical giant cells contained more than five round nuclei (Fig. 3A). Immunocytochemically, these multinucleated giant cells were located in the adluminal compartment of the epithelium above the ZO-1-positive BTB and surrounded by espin, a component of the ectoplasmic specialization (ES) between Sertoli cells and spermatids (Fig. 3D, F) (2). These findings indicated that the multinucleated giant cells had originated from a cohort of spermatids that could not be properly separate during mitosis and meiosis. On day 28 of treatment with leuprorelin, the thickness of the seminiferous epithelium became markedly reduced compared with control rats, and relatively large spermatocytes were directly exposed to the lumen (Fig. 2J). The multinucleated giant cells were no longer frequently observed in the epithelium.

In contrast to the drastic changes in the seminiferous tubules of rats receiving the leuprorelin depot, no apparent changes were discerned in those of rats receiving the degarelix depot until day 7 of treatment (Fig. 2C, E, G, see also Fig. 3E). Only a small amount of premature spermatids had detached from the seminiferous epithelium and were observed in the lumen (Fig. 2G, arrows), and no multinucleated giant cells were observed in the testis of degarelix-treated rats throughout the experimental period. However, on day 14 of treatment with degarelix, the diameter of seminiferous tubules and the epithelium thickness were apparently reduced (Fig. 2I). Atrophic changes in the seminiferous tubules progressed until day 28, and the mean diameter of the seminiferous tubules became about half of that in control rats (Fig. 2K; see also Table 1). In the seminiferous epithelium on day 28 of treatment with degarelix, mature spermatozoa were not found, and relatively large spermatocytes were located on the surface of the epithelium (Fig. 2K), as observed in the seminiferous epithelium on day 28 of treatment with leuprorelin (Fig. 2J).

Semiquantitative evaluation confirmed the changes in the diameter of seminiferous tubules and the frequency of occurrence of multinucleated giant cells.

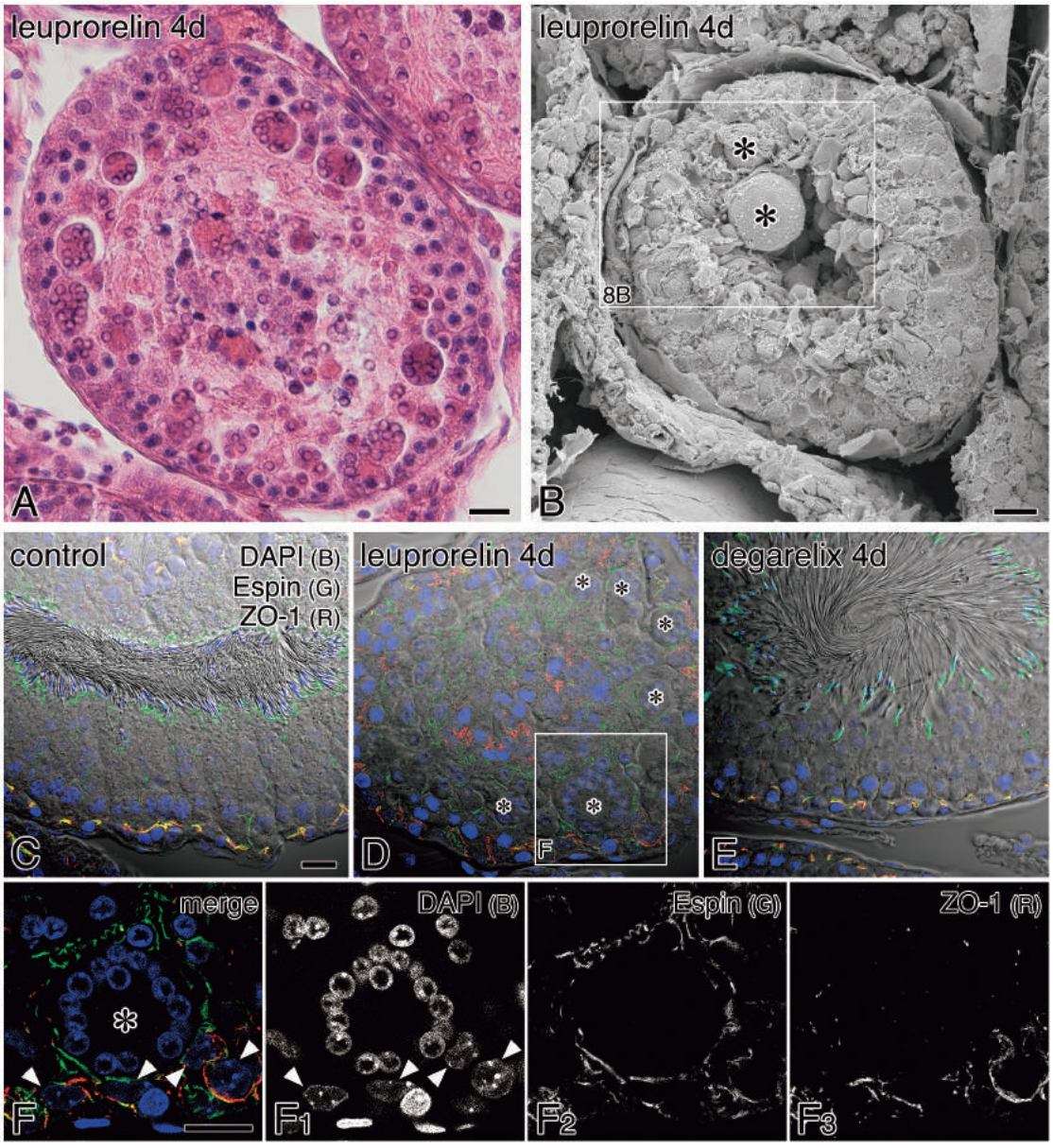

Fig. 3 Multinucleated giant cells in the seminiferous epithelium of rats on day 4 after administration of a depot formulation of GnRH agonist leuprorelin. (**A**) Magnified view of the seminiferous tubule indicated in Fig. 2D. Numerous giant cells containing multiple nuclei were observed in the tubule. Bar = 20 μm. (**B**) Similar seminiferous tubule observed by SEM. Extraordinarily large cells (asterisks) were observed in the tubule. The boxed area indicated with the white line is enlarged and shown in Fig. 8B. Bar = 20 μm. (**C**–**E**) Seminiferous epithelium immunostained with anti-espin (green pseudocolor) and anti-ZO-1 (red pseudocolor) antibodies observed under a confocal laser scanning microscope. Nuclei were stained with DAPI (blue pseudocolor). Differential interference contrast (DIC) images acquired by a transmission detector are overlaid on the corresponding immunostained images. Note the massive exfoliation of spermatids in the lumen and occurrence of numerous multinucleated giant cells (asterisks) in the seminiferous epithelium of the leuprorelin-treated rat on day 4 of treatment (D). Seminiferous epithelia of a control rat (C) and degarelix-treated rat on day 4 of treatment (E) appeared to be properly organized, including differentiated spermatids with an elongated tail. The boxed area indicated with the white line in (D) is enlarged and shown in (F). Bar = 20 μm. (**F**) Magnified view of the multinucleated giant cell (asterisk) indicated in (D). A merged image of DAPI (blue), and anti-espin (green) and anti-ZO-1 antibody staining is shown in the left panel. Individual signals for DAPI, espin, and ZO-1 in black and white are separately shown in F_1, F_2, and F_3, respectively. The giant cell containing more than 10 nuclei (blue in F; white in F_1) was surrounded by the signal for espin (red in F; white in F_2) and located above the BTB. Note that the BTB indicated by signals of both espin (red in F; white in F_2) and ZO-1 (green in F; white in F_3) was preserved between the adjacent Sertoli cells (white arrowheads) at the basal area of the seminiferous epithelium. Bar = 20 μm.

The giant cells first appeared in the seminiferous tubules of rats receiving the leuprorelin depot on day 1, and the frequency of occurrence peaked from day 4 to 7, while giant cells were hardly observed in rats receiving the degarelix depot throughout the experimental period (Table 1).

Differences in the ultrastructure of the seminiferous epithelium between experimental groups at 7 days after receiving GnRH agonist leuprorelin and antagonist degarelix

Because the differences in weight and histology of the testis between experimental groups receiving the GnRH agonist or antagonist were mostly manifested on day 7 after the onset of treatment, we next compared the ultrastructure of the seminiferous epithelium in both groups of rats on day 7 after receiving leuprorelin and degarelix depots.

Occurrence of the multinucleated giant cells and exfoliation of the spermatids were confirmed on a semithin section of the testis on day 7 of continuous treatment with leuprorelin correlatively by light microscopy (Fig. 4A) and BSE-mode SEM (Fig. 4B–D). In the seminiferous epithelium, mature spermatozoa with a distinct tail were hardly found, and numerous premature spermatids and multinucleated giant cells had detached from the epithelium and were observed in the lumen (Fig. 4C). A profile of multinucleated giant cells mostly contained 5–10 nuclei and other organelles characteristic of the spermatid, such as the Golgi apparatus and fragments of acrosomal vesicles (Fig. 4D), indicating that a giant cell consisted of incompletely separated spermatids. The chromatin atypically condensed into a ring at the peripheral region of some nuclei in giant cells (Fig. 4D, arrowheads), suggesting that the giant cells were under degeneration, probably by apoptotic processes (53). The cellular processes of Sertoli cells were markedly retracted from the apical region of the seminiferous epithelium, while the luminal spaces of the seminiferous tubule reciprocally intruded between the spermatids and multinucleated giant cells, thus accelerating premature exfoliation of spermatogenic cells from the epithelium. However, the basal part of Sertoli cells was seemingly intact, where the BTB between adjacent Sertoli cells appeared functional because the intercellular junctions including tight junction and basal ectoplasmic specialization (basal ES) were properly preserved (Fig. 4E, arrowheads). Small lipid droplets were occasionally discerned in the basal cytoplasm of Sertoli cells (Fig. 4E).

In contrast to the seminiferous epithelium of leuprorelin-treated rats described above, no multinucleated giant cells appeared in the seminiferous epithelium of rats on day 7 after receiving the degarelix depot. Spermatogonia, spermatocytes, and spermatids with normal appearances were laid in order as a cellular pile in the epithelium (Fig. 5). The spaces between the piles of spermatogenic cells, including maturating spermatids extending a tail, were properly filled with the cytoplasm of cellular processes of Sertoli cells (Fig. 5A–C). Between Sertoli cells in the basal compartment of the seminiferous epithelium, numerous mitotic spermatogonia surrounded with conspicuous extracellular spaces were frequently encountered (Fig. 5D, E). These findings suggested that treatment with the depot of degarelix for 7 days did not induce atrophic changes in the seminiferous tubules or impair the mitotic division of spermatogonia.

Chronic changes in seminiferous tubules by treatment with GnRH antagonist degarelix

Although no apparent changes were discerned in the seminiferous tubules of rats until day 7 after receiving the degarelix depot, atrophic changes subsequently manifested in the seminiferous epithelium of degarelix-treated rats.

In the seminiferous epithelium of rats on day 14 after receiving the degarelix depot, only a few maturating sperms were found (Fig. 6A, B). Between the perpendicularly aligned spermatids, there were anomalous spaces intruded from the tubular lumen (Fig. 6C). The adjacent Sertoli cells appeared to be still interconnected by the intercellular junctions at the basal compartment of the epithelium (Fig. 6D, arrowheads), and spermatogonia beneath the BTB also exhibited a normal appearance. Large lipid droplets were frequently observed above the nucleus of Sertoli cells located at the basal area of the seminiferous tubule (Fig. 6D, E).

The retraction of the cellular processes of Sertoli cells toward the basal compartment was more prominent in the seminiferous epithelium of rats on day 28 after receiving the degarelix depot (Fig. 7A–C). The spermatocytes that had recently translocated from the basal compartment to the upper compartment across the BTB were often exposed directly to the luminal space of seminiferous tubules (Fig. 7C, arrowheads). Premature spermatids appeared to be exfoliated from the epithelial wall into the lumen by prolonged treatment with the degarelix depot, although the spermatids did not form multinucleated giant cells, but were apparently mono- or bi-nucleated cells (Fig. 7C, black arrows). Even at this time

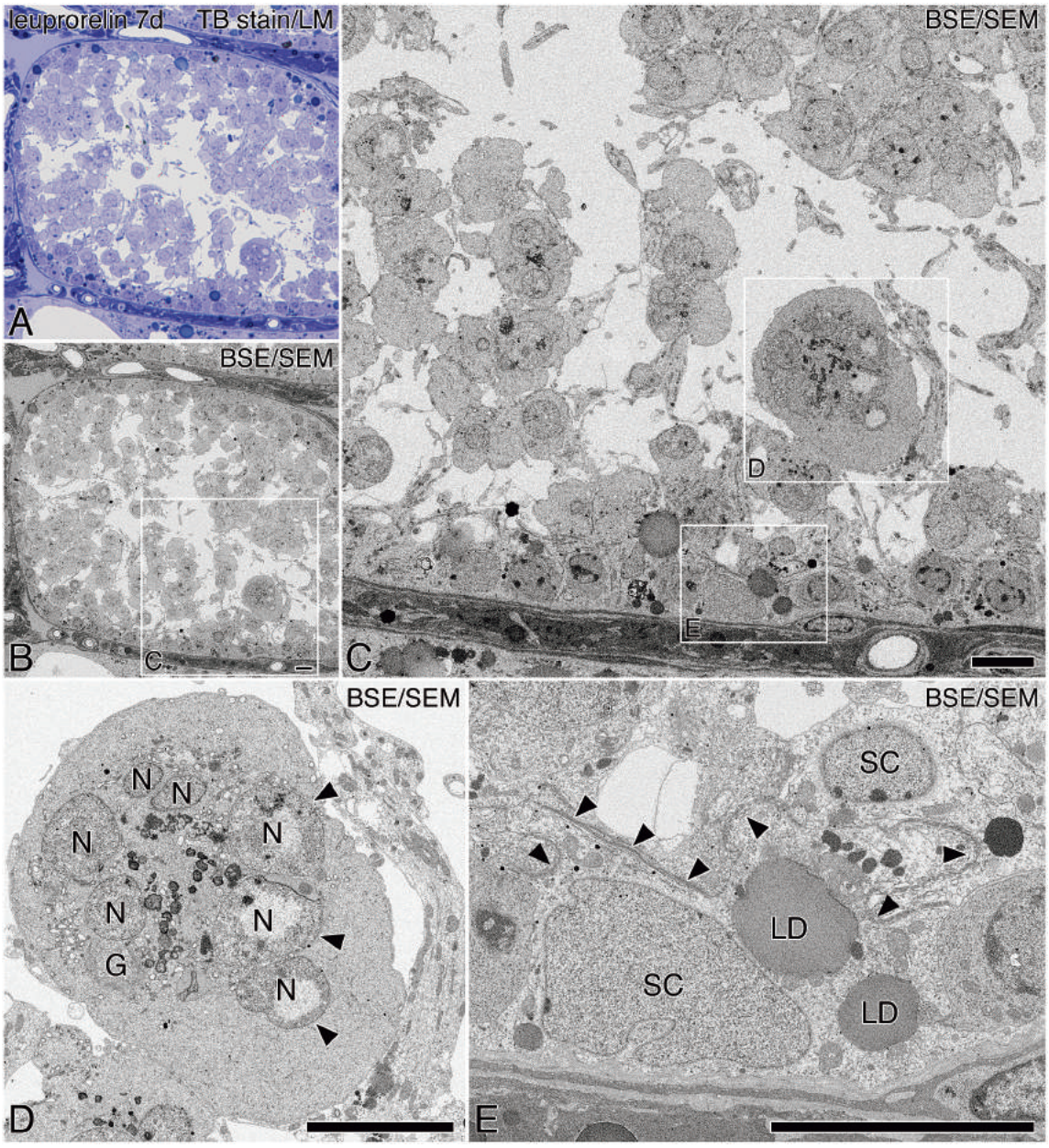

Fig. 4 Seminiferous epithelium of a rat on day 7 after administration of a depot formulation of GnRH agonist leuprorelin observed by correlative light and scanning electron microscopy. (**A**) Toluidine blue-stained semithin section of the rat testis observed by light microscopy. (**B**) The identical area in (A) on the semithin section observed by BSE-mode SEM. Note that the wide area of the specimen observed by light microscopy could be correlatively imaged at the electron microscopic level without any obstruction. The boxed area indicated with the white line is enlarged and shown in (C). Bar = 10 μm. (**C**) Seminiferous epithelium observed by BSE-mode SEM at a higher magnification. Note the massive detachment of round/premature spermatids from the epithelium. The boxed areas indicated with white lines are enlarged and shown in (D) and (E). Bar = 10 μm. (**D**) Magnified view of the multinucleated giant cell indicated in (C). Note that numerous electron-dense structures, probably derived from acrosomes, were surrounded by the multiple profiles of nuclei (N). Note that chromatin was peripherally condensed in some nuclei (arrowheads). G: Golgi apparatus. Bar = 10 μm. (**E**) Higher magnification of the boxed area indicated in (C). In the basal cytoplasm of Sertoli cells (SC), lipid droplets (LD) were occasionally observed. Note that adjacent Sertoli cells apparently adhered firmly to each other at the basal compartment of the epithelium by continuous intercellular junctions (arrowheads) including tight junction and basal ES. Bar = 10 μm.

point, the spermatogonia beneath the BTB appeared to be intact (Fig. 7D). Accumulation of lipid droplets in Sertoli cells became more prominent on day 28 compared with day 14, and the lipid droplets were apparently translocated near to the luminal space (Fig. 7C, D). Exposure of larger spermatocytes to the lumen and accumulation of lipid droplets were also observed in the seminiferous epithelium on day 28 of treatment with leuprorelin, although the lipid droplets in leuprorelin-treated rats were much small-

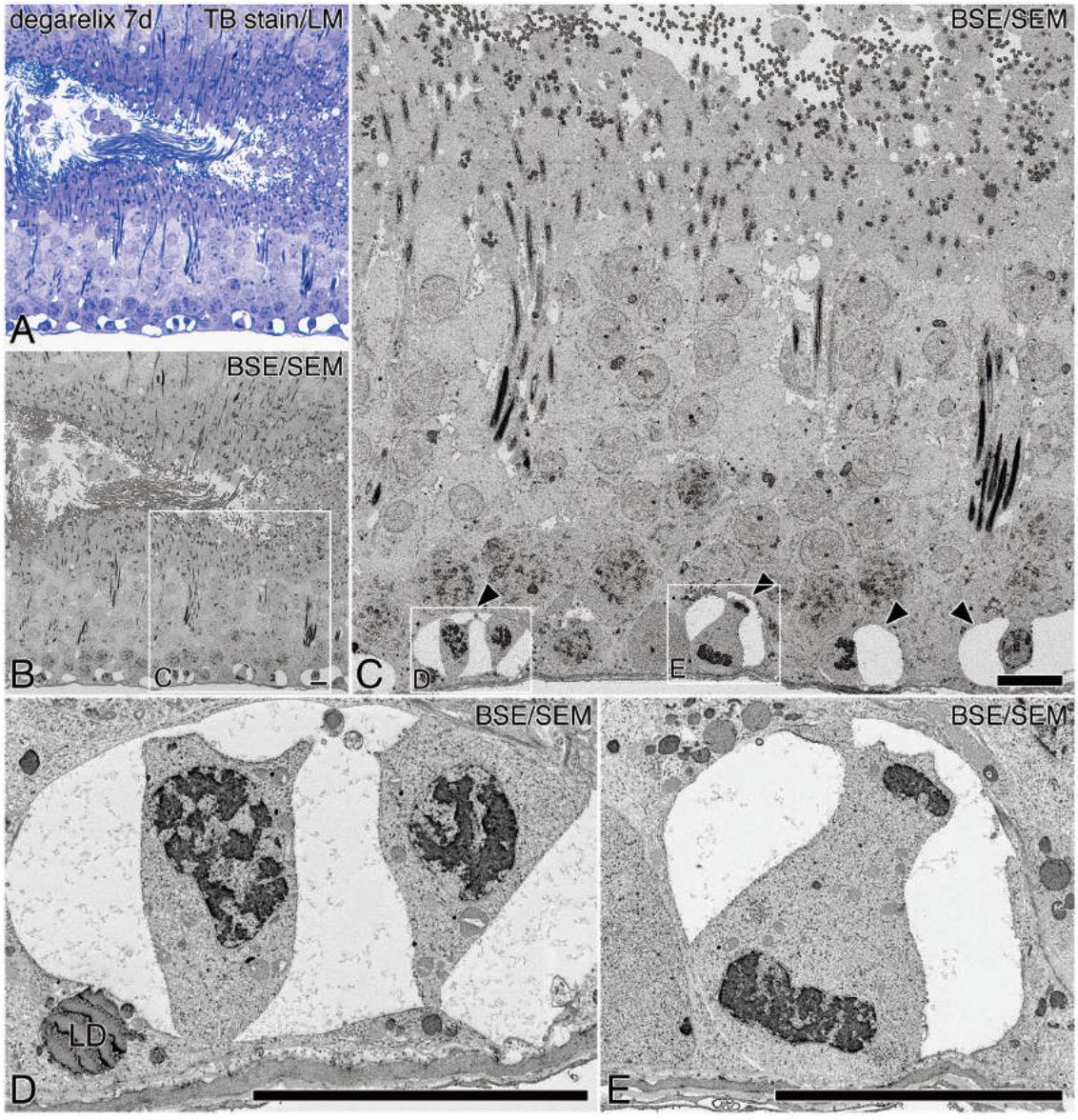

Fig. 5 Seminiferous epithelium of a rat on day 7 after administration of a depot formulation of GnRH antagonist degarelix observed by correlative light and scanning electron microscopy. (**A**) Toluidine blue-stained semithin section of the rat testis observed by light microscopy. (**B**) The identical area in (A) on the semithin section observed by BSE-mode SEM. The boxed area indicated with the white line is enlarged and shown in (C). Bar = 10 μm. (**C**) Seminiferous epithelium observed by BSE-mode SEM at a higher magnification. The epithelium was properly filled with Sertoli and spermatogenic cells of normal appearances. Differentiating spermatids with a tail were also observed. Note the spermatogonia during mitosis at the base of the epithelium (arrowheads). The boxed areas indicated with white lines are enlarged and shown in (D) and (E). Bar = 10 μm. (**D**) Magnified view of the pair of spermatogonia indicated in (C). Note that these spermatogonia were surrounded by a common space at the base of the epithelium, probably just after mitosis. LD: lipid droplet. Bar = 10 μm. (**E**) Magnified view of the spermatogonia during mitosis indicated in (C). Two clusters of condensed chromatin were located separately at the two opposite poles of the cell. Bar = 10 μm.

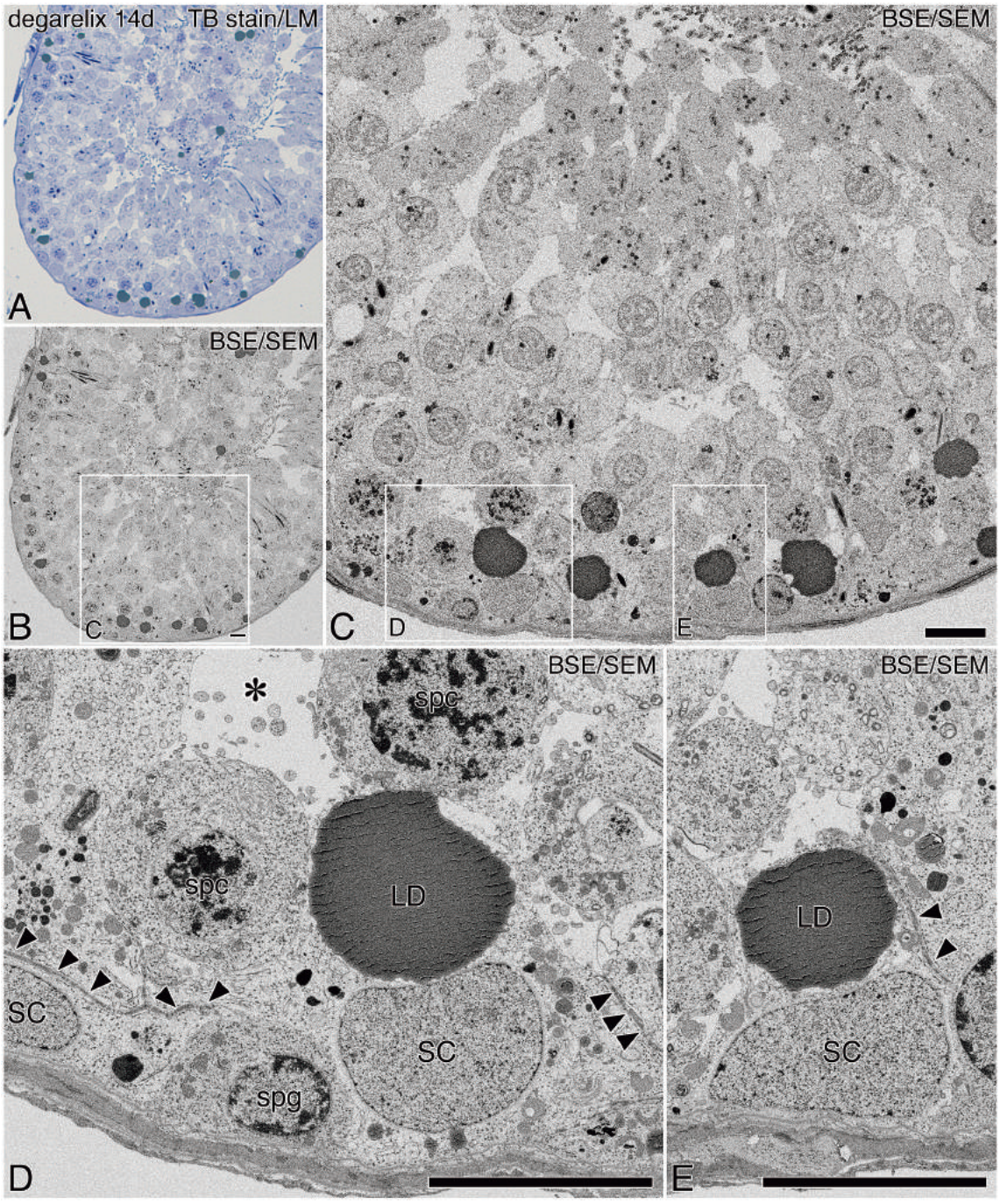

Fig. 6 Seminiferous epithelium of a rat on day 14 after administration of a depot formulation of GnRH antagonist degarelix observed by correlative light and scanning electron microscopy. (**A**) Toluidine blue-stained semithin section of the rat testis observed by light microscopy. (**B**) The identical area in (A) on the semithin section observed by BSE-mode SEM. The boxed area indicated with the white line is enlarged and shown in (C). Bar = 10 μm. (**C**) Seminiferous epithelium observed by BSE-mode SEM at a higher magnification. Anomalous spaces appeared between round spermatids in the epithelium. Note prominent accumulation of lipid droplets in the basal area of the epithelium. The boxed areas indicated with white lines are enlarged and shown in (D) and (E). Bar = 10 μm. (**D**) Higher magnification of the boxed area indicated in (C). Note the large lipid droplet (LD) in the basal cytoplasm of a Sertoli cell (SC). Adjacent Sertoli cells apparently adhered firmly to each other at the basal compartment of the epithelium by continuous tight junctions (arrowheads), although luminal spaces (asterisk) intruded just above spermatocytes (spc) between Sertoli cells. The spermatogonia (spg) observed below the intercellular junction appeared to be intact. Bar = 10 μm. (**E**) Magnified view of another lipid droplet (LD) in the Sertoli cell (SC) shown in (C). Tight junctions (arrowheads) were continuously formed between adjacent Sertoli cells. Bar = 10 μm.

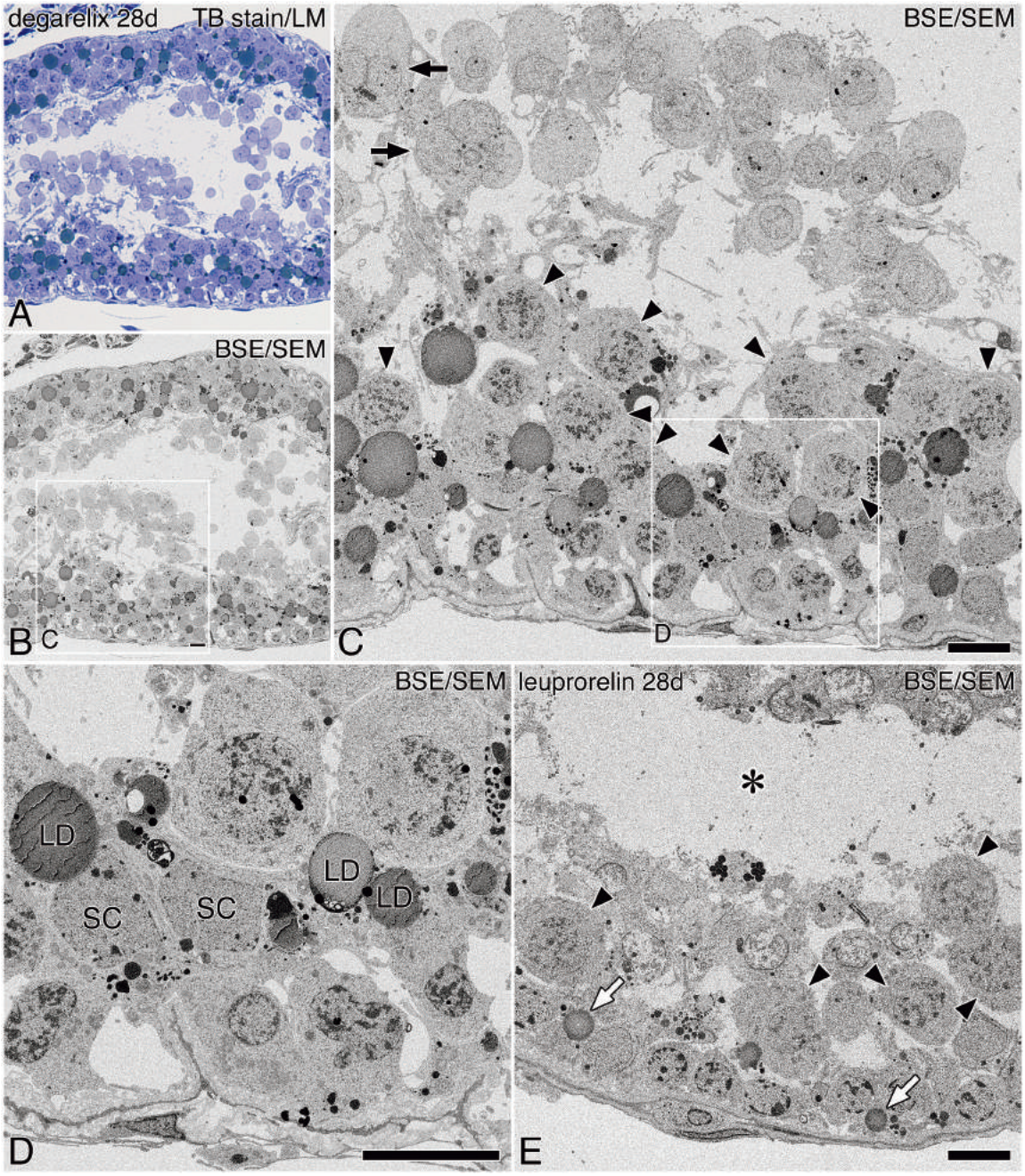

Fig. 7 Seminiferous epithelium of the rats on day 28 after administration of the depot formulations of GnRH antagonist degarelix (A–D) and agonist leuprorelin (E) observed by correlative light and scanning electron microscopy. (**A**) Toluidine blue-stained semithin section of the degarelix-treated rat testis on day 28 observed by light microscopy. (**B**) The identical area in (A) on the semithin section observed by BSE-mode SEM. The boxed area indicated with the white line is enlarged and shown in (C). Bar = 10 μm. (**C**) Seminiferous epithelium observed by BSE-mode SEM at a higher magnification. The height of the epithelium was markedly reduced. Round spermatids had largely exfoliated from the epithelium, and spermatocytes (arrowheads) located just above the Sertoli cells were exposed directly to the lumen. Note the binucleated round spermatids (black arrows) detached from the epithelium. The boxed area indicated with the white line is enlarged and shown in (D). Bar = 10 μm. (**D**) Higher magnification of the boxed area indicated in (C). Note that the accumulation of lipid droplets (LD) in the basal cytoplasm of a Sertoli cell (SC) became more prominent compared with that on day 14 of treatment (Fig. 6). Bar = 10 μm. (**E**) Seminiferous epithelium observed on day 28 of leuprorelin treatment by BSE-mode SEM at the same magnification in (C). Lipid droplets (white arrows) had also accumulated in the basal cytoplasm of Sertoli cells, but less prominently compared with that in degarelix-treated rats (C). Note that the height of the epithelium was highly reduced, and spermatocytes (arrowheads) were largely exposed to the luminal space (asterisk). Bar = 10 μm.

er and less frequently encountered (Fig. 7E, white arrows).

Changes in the 3D ultrastructure of Sertoli cells in the seminiferous epithelium after administration of depot formulations of GnRH analogues

Observations of KOH-digested testicular tissues by SEM revealed the 3D ultrastructure of Sertoli cells in leuprorelin- and degarelix-treated rats (Fig. 8). In the seminiferous epithelium of control rats, apical cytoplasm of Sertoli cells was well extended between the piles of spermatogenic cells (Fig. 8A). The apical cytoplasmic processes appeared to be well preserved between spermatogenic cells in the seminiferous epithelium of degarelix-treated rats until 7 days after the onset of treatment (Fig. 8C), while the cytoplasmic processes of Sertoli cells in leuprorelin-treated rats were largely deformed and the height of the epithelium was markedly reduced during the first week of treatment (Fig. 8B, D). On day 28 of treatment, the cytoplasmic processes of Sertoli cells in both degarelix (Fig. 8E)- and leuprorelin (Fig. 8F)-treated rats were prominently deformed and filled the large part of the seminiferous epithelium instead of spermatids.

In summary, the seminiferous epithelium became promptly atrophic by massive exfoliation of premature spermatids upon administration of the depot formulation of GnRH agonist leuprorelin, whereas the atrophic changes much slowly proceeded in the seminiferous epithelium of GnRH antagonist degarelix-treated rats, even though enormous loss of spermatids from seminiferous tubules occurred as a common consequence after long term treatment with each GnRH analogue.

DISCUSSION

Depot formulations of GnRH analogues that chronically suppress the production of sex steroids in gonads have been widely used for the treatment of androgen/estrogen-sensitive tumors and diseases such as prostate cancer, uterine leiomyoma, prepubertal maturation, and endometriosis (1, 11, 14, 39). The present study clearly described the histological and cytological changes in the seminiferous tubules of male rats after receiving depot formulations of two opposing types of GnRH analogues, agonist leuprorelin and antagonist degarelix. Similar to earlier studies of GnRH agonists (35, 61) and antagonists (4, 40, 51), long term treatments with GnRH analogues, both leuprorelin and degarelix in the present study, resulted in a similar atrophic consequence of the seminiferous tubules. The wet weight of a testis and the mean diameter of seminiferous tubules were markedly reduced at 4 weeks after administration of both leuprorelin and degarelix depots. At this time point, the height of the seminiferous epithelium was markedly reduced, and most spermatids had disappeared from the adluminal compartment of the seminiferous epithelium.

However, the changes observed in the seminiferous tubules during the first 7 days after administration were quite different between agonist- and antagonist-treated animals. Massive exfoliation (sloughing) of premature spermatids into the tubular lumen and anomalous multinucleated giant cells appeared specifically in the seminiferous epithelium of GnRH agonist-treated rats, but not in that of GnRH antagonist-treated rats. Exfoliation of premature and/or abnormal spermatids has been reported in numerous pathological states of seminiferous tubules (18, 57). The anomalous release of extraordinary amounts of premature spermatids putatively results from inadequate dissociation of the intercellular junctional complex between spermatids and Sertoli cells. At the adluminal compartment of the seminiferous epithelium, unique intercellular junctional complexes, the apical ES and tubulobulbar complex, tether the differentiating spermatids to Sertoli cells during spermiogenesis (21, 42, 43, 54, 65). Dissociation of the intercellular junctions at the adequate timing is essential for proper spermiation, a physiological step to release mature spermatozoa into the tubular lumen, while that at an inadequate timing presumably results in pathological states such as the massive exfoliation of premature spermatids (30, 31, 33, 63).

In addition to the massive exfoliation of premature spermatids, multinucleated giant cells were frequently observed in the seminiferous epithelium of GnRH agonist-treated animals, but not in that of GnRH antagonist-treated animals throughout the experimental period. The occurrence of multinucleated giant cells has been reported in several experimental/pathological states of seminiferous tubules (6, 17, 38), including rat seminiferous tubules at 7 days after administration of a depot formulation of GnRH agonist zoladex (56). The most well-described experimental condition that reproducibly induces multicellular giant cells in the seminiferous epithelium is administration of a potential contraceptive drug, adjudin. Administration of adjudin to male rats promptly induces both exfoliation of spermatids and the occurrence of multinucleated giant cells in the seminiferous tubules (9, 10), which are similar to the changes in the seminiferous epithelium shortly after

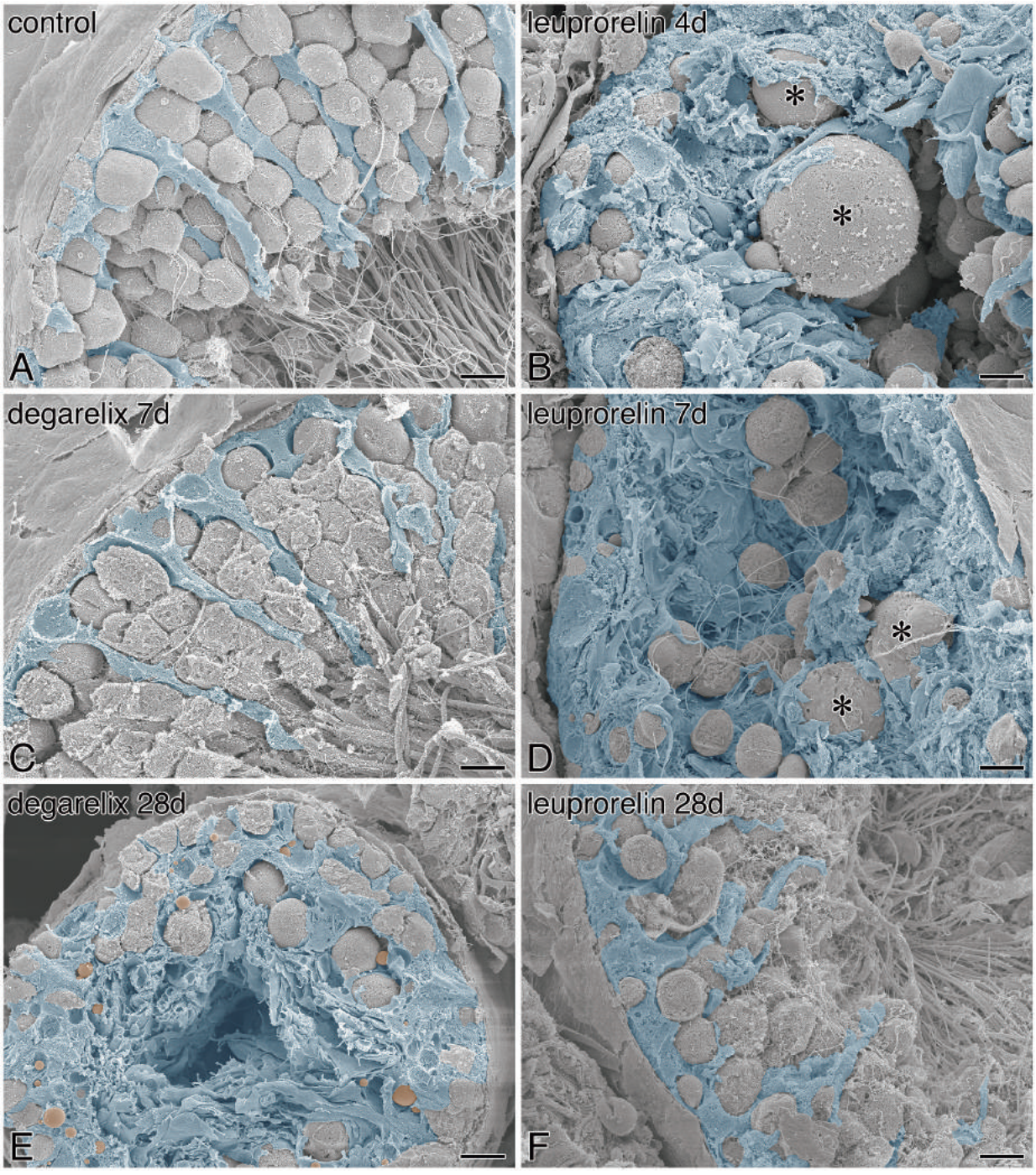

Fig. 8 3D ultrastructure of Sertoli cells in the seminiferous epithelium of leuprorelin (B, D, F)- and degarelix (C, E)-treated rats on day 4 (B), day 7 (C, D), and day 28 (E, F) of treatments. The seminiferous epithelium of a control rat is shown in (A). After preparation according to the simple KOH digestion method by Ushiki and Ide (55), testicular tissues were observed by SEM at the same magnification. The apical cytoplasm of Sertoli cells (blue) in the seminiferous epithelium of leuprorelin-treated rats had promptly deformed on day 4 from the onset of treatment (B), whereas that of degarelix-treated rats was still properly extended between the piles of spermatocytes and spermatids even on day 7 (C), which was similar to that in control rats (A). On day 28 of treatment, the apical cytoplasm of Sertoli cells of both degarelix (E)- and leuprorelin (F)-treated rats had largely retracted and deformed, and large spermatocytes were located near the lumen of seminiferous tubules. Note the extraordinarily large giant cells observed on days 4 and 7 of leuprorelin treatment (asterisks). On day 28 of degarelix treatment, spherical lipid droplets were frequently observed through the partially cracked cytoplasm of Sertoli cells (E; orange). Bars = 10 μm.

administration of the leuprorelin depot in the present study. Because proper separation of spermatids derived from a common cohort presumably needs adequate structural support by adjacent Sertoli cells (30), administration of adjudin putatively impairs the intercellular adhesion machinery between Sertoli cells and spermatogenic cells, especially the apical ES, thus resulting in premature release and inadequate separation of differentiating spermatids in seminiferous tubules (25, 26).

The transient but explosive increase in secretion of pituitary gonadotropins and testosterone, which only occurs in the acute phase of GnRH agonist treatment (34, 36), possibly exerts similar effects on the sealing properties of intercellular junctions between Sertoli cells and spermatogenic cells. In particular, one of the gonadotropins, FSH, suppresses the nonclassical signaling pathway evoked by testosterone that maintains the function of the apical ES, leading to a reduction of intercellular adhesion between Sertoli cells and differentiating spermatids (48, 58). Under the influence of excessive FSH shortly after administration of a GnRH agonist, a cohort of interconnected spermatocytes in meiosis is possibly translocated prematurely through the loosened BTB to the adluminal compartment where the cohort forms an anomalous multinucleated giant cell because of cytokinetic separation failure. A report demonstrating that degenerating polynucleated cells occur in the seminiferous tubules of male rats treated continuously with highly purified human FSH, but not in those treated with testosterone alone (3), supports the involvement of excessive FSH in the pathogenesis of histological changes specifically seen in the acute phase of GnRH agonist treatment in the present study.

In contrast to the acute changes described above, the histopathological consequences in the seminiferous epithelium at 28 days after administration of the leuprorelin and degarelix depots resembled each other. Both round and elongated spermatids were almost lost in the seminiferous epithelium, and relatively larger spermatocytes before the final cell division of meiosis were exposed directly to the tubular lumen. Thus, the fate of the differentiating spermatids residing in the seminiferous epithelium at the onset of treatment with degarelix remains to be elucidated. Depletion of testosterone caused by the continuous influence of GnRH analogues presumably blocks spermiogenesis and spermiation around stages VII/VIII (32, 51), and the persistent germ cells in the seminiferous epithelium are prone to apoptosis (49, 50). Progressive accumulation of lipid droplets in Sertoli cells during long term treatment with GnRH analogues, especially with antagonist degarelix observed in the present study, suggests the acceleration of phagocytic disposal of residual and/or defective spermatids by the surrounding Sertoli cells (12, 27, 62).

As a common consequence after prolonged treatments with both the GnRH agonist and antagonist, the height of the seminiferous epithelium was markedly reduced, supposedly resulting from the retraction of apical cytoplasm of Sertoli cells and the latently progressive liberation of premature spermatids. Previous studies have demonstrated that loss of gonadotropins and/or testosterone not only reduces the adhesive strength of intercellular junctions between Sertoli and spermatogenic cells, but also affects the organization of cytoskeletal elements in Sertoli cells (47). Because Sertoli cells provide a niche for spermatogenesis, disorganization of the cytoskeleton in the apical cytoplasm of Sertoli cells crucially leads to abrupt exit of spermatids from the seminiferous epithelium above the BTB promptly after meiosis (18, 47, 52, 60). Regression of spermatogenesis at late meiosis due to loss of plasma gonadotropins and intratesticular testosterone (13, 58) also foregrounds the residual large spermatocytes directly facing the lumen, as observed in the seminiferous epithelium at the late phase after administration of both GnRH agonist leuprorelin and antagonist degarelix depots.

In summary, the present study clearly demonstrated the differences in the effects of two opposing types of GnRH analogues, the agonist leuprorelin and antagonist degarelix, on the rat seminiferous epithelium. The GnRH agonist promptly induced massive exfoliation and inadequate separation of premature spermatids by its own hyperstimulatory effect during the early phase after administration, whereas the GnRH antagonist caused no apparent changes shortly after administration, although the histopathological consequences after long term treatment with both types of GnRH analogues were similarly atrophic changes and regression of spermatogenesis in seminiferous tubules. The comparison of the effects of the two substantially different types of GnRH analogues could possibly contribute to making more appropriate choices of GnRH analogues for clinical use to minimize adverse effects on spermatogenesis in the testis when reproductive functions should be preserved. For this purpose, recovery processes of the seminiferous epithelium after ceasing treatment with long-acting GnRH analogues should be compared further in detail.

Acknowledgments

The authors thank Yukari Dan of Hitachi High-Technologies for technical support with cold field emission-type SEM. We also thank Mitchell Arico from Edanz Group (www.edanzediting.com/ac) for editing a draft of this manuscript.

This work was supported in part by Grants-in-Aid for Scientific Research (C) from the Japanese Society for the Promotion of Science (JSPS) (17K08505 to T.W. and 16K08458 to D.K.).

REFERENCES

1. Barbieri RL (1992) Clinical applications of GnRH and its analogues. *Trends Endocrinol Metab* **3**, 30–34.
2. Bartles JR, Wierda A and Zheng L (1996) Identification and characterization of espin, an actin-binding protein localized to the F-actin-rich junctional plaques of Sertoli cell ectoplasmic specializations. *J Cell Sci* **109**, 1229–1239.
3. Bartlett JM, Weinbauer GF and Nieschlag E (1989) Differential effects of FSH and testosterone on the maintenance of spermatogenesis in the adult hypophysectomized rat. *J Endocrinol* **121**, 49–58.
4. Bhasin S, Fielder T, Peacock N, Sod-Moriah UA and Swerdloff RS (1988) Dissociating antifertility effects of GnRH-antagonist from its adverse effects on mating behavior in male rats. *Am J Physiol* **254**, E84–91.
5. Bliss SP, Navratil AM, Xie J and Roberson MS (2010) GnRH signaling, the gonadotrope and endocrine control of fertility. *Front Neuroendocrinol* **31**, 322–340.
6. Bolor H, Wakasugi N, Zhao WD and Ishikawa A (2006) Detection of quantitative trait loci causing abnormal spermatogenesis and reduced testis weight in the small testis (Smt) mutant mouse. *Exp Anim* **55**, 97–108.
7. Brogden RN, Buckley MM and Ward A (1990) Buserelin. A review of its pharmacodynamic and pharmacokinetic properties, and clinical profile. *Drugs* **39**, 399–437.
8. Broqua P, Riviere PJ, Conn PM, Rivier JE, Aubert ML and Junien JL (2002) Pharmacological profile of a new, potent, and long-acting gonadotropin-releasing hormone antagonist: degarelix. *J Pharmacol Exp Ther* **301**, 95–102.
9. Cheng CY (2014) Toxicants target cell junctions in the testis: Insights from the indazole-carboxylic acid model. *Spermatogenesis* **4**, e981485.
10. Cheng CY, Silvestrini B, Grima J, Mo MY, Zhu LJ, Johansson E, Saso L, Leone MG, Palmery M and Mruk D (2001) Two new male contraceptives exert their effects by depleting germ cells prematurely from the testis. *Biol Reprod* **65**, 449–461.
11. Conn PM, and Crowley WF (1994) Gonadotropin-releasing hormone and its analogs. *Annu Rev Med* **45**, 391–405.
12. Flickinger C (1978) Effects of testosterone enanthate on the structure of the male reproductive tract of the rat. *Anat Rec* **192**, 555–584.
13. Franca LR, Parreira GG, Gates RJ and Russell LD (1998) Hormonal regulation of spermatogenesis in the hypophysectomized rat: quantitation of germ-cell population and effect of elimination of residual testosterone after long-term hypophysectomy. *J Androl* **19**, 335–342
14. Griesinger G, Felberbaum R and Diedrich K (2005) GnRH-antagonists in reproductive medicine. *Arch Gynecol Obstet* **273**, 71–78.
15. Griswold MD, ed. (2015) *Sertoli Cell Biology*. Elsevier, Amsterdam, Netherlands.
16. Hess RA and de Franca LR (2008) Spermatogenesis and cycle of the seminiferous epithelium. In: *Molecular Mechanisms in Spermatogenesis*. *Adv Exp Med Biol* **636**, 1–15. Cheng CY, ed. Springer, New York, NY.
17. Holstein AF and Eckmann C (1986) Multinucleated spermatocytes and spermatids in human seminiferous tubules. *Andrologia* **18**, 5–16.
18. Johnson KJ (2014) Testicular histopathology associated with disruption of the Sertoli cell cytoskeleton. *Spermatogenesis* **4**, e979106.
19. Kitahara K, Sakai Y, Hosaka M, Hira Y, Kakizaki H and Watanabe T (2007) Effects of a depot formulation of the GnRH agonist leuprorelin on the ultrastructure of male rat pituitary gonadotropes. *Arch Histol Cytol* **70**, 79–93.
20. Koga D, Kusumi S, Shodo R, Dan Y and Ushiki T (2015) High-resolution imaging by scanning electron microscopy of semithin sections in correlation with light microscopy. *Microscopy (Oxf)* **64**, 387–394.
21. Kopera IA, Bilinska B, Cheng CY and Mruk DD (2010) Sertoli-germ cell junctions in the testis: a review of recent data. *Philos Trans R Soc Lond B Biol Sci* **365**, 1593–1605.
22. Leblond CP and Clermont Y (1952) Definition of the stages of the cycle of the seminiferous epithelium in the rat. *Ann N Y Acad Sci* **55**, 548–573.
23. McArdle CA, Franklin J, Green L and Hislop JN (2002) Signalling, cycling and desensitisation of gonadotrophin-releasing hormone receptors. *J Endocrinol* **173**, 1–11.
24. Millar RP, Lu ZL, Pawson AJ, Flanagan CA, Morgan K and Maudsley SR (2004) Gonadotropin-releasing hormone receptors. *Endocr Rev* **25**, 235–275.
25. Mok KW, Mruk DD, Lie PP, Lui WY and Cheng CY (2011) Adjudin, a potential male contraceptive, exerts its effects locally in the seminiferous epithelium of mammalian testes. *Reproduction* **141**, 571–580.
26. Mruk DD and Cheng CY (2011) Testin and actin are key molecular targets of adjudin, an anti-spermatogenic agent, in the testis. *Spermatogenesis* **1**, 137–146.
27. Nakanishi Y and Shiratsuchi A (2004) Phagocytic removal of apoptotic spermatogenic cells by Sertoli cells: mechanisms and consequences. *Biol Pharm Bull* **27**, 13–16.
28. Namimatsu S, Ghazizadeh M and Sugisaki Y (2005) Reversing the effects of formalin fixation with citraconic anhydride and heat: a universal antigen retrieval method. *J Histochem Cytochem* **53**, 3–11.
29. Naor Z (2009) Signaling by G-protein-coupled receptor (GPCR): studies on the GnRH receptor. *Front Neuroendocrinol* **30**, 10–29.
30. O'Donnell L (2014) Mechanisms of spermiogenesis and spermiation and how they are disturbed. *Spermatogenesis* **4**, e979623.
31. O'Donnell L, McLachlan RI, Wreford NG, de Kretser DM and Robertson DM (1996) Testosterone withdrawal promotes stage-specific detachment of round spermatids from the rat seminiferous epithelium. *Biol Reprod* **55**, 895–901.
32. O'Donnell L, McLachlan RI, Wreford NG and Robertson DM (1994) Testosterone promotes the conversion of round spermatids between stages VII and VIII of the rat spermatogenic cycle. *Endocrinology* **135**, 2608–2614.
33. O'Donnell L, Nicholls PK, O'Bryan MK, McLachlan RI and Stanton PG (2011) Spermiation: The process of sperm release. *Spermatogenesis* **1**, 14–35.
34. Okada H, Heya T, Ogawa Y, Toguchi H and Shimamoto T

(1991) Sustained pharmacological activities in rats following single and repeated administration of once-a-month injectable microspheres of leuprolide acetate. *Pharm Res* **8**, 584–587.
35. Pelletier G, Cusan L, Auclair C, Kelly PA, Desy L and Labrie F (1978) Inhibition of spermatogenesis in the rat by treatment with [D-Ala^6, Des-Gly-NH$_2^{10}$] LHRH ethylamide. *Endocrinology* **103**, 641–643.
36. Plosker GL and Brogden RN (1994) Leuprorelin. A review of its pharmacology and therapeutic use in prostatic cancer, endometriosis and other sex hormone-related disorders. *Drugs* **48**, 930–967.
37. Ramaswamy S and Weinbauer GF (2014) Endocrine control of spermatogenesis: Role of FSH and LH/ testosterone. *Spermatogenesis* **4**, e996025.
38. Ren HP and Russell LD (1991) Clonal development of interconnected germ cells in the rat and its relationship to the segmental and subsegmental organization of spermatogenesis. *Am J Anat* **192**, 121–128.
39. Rick FG and Schally AV (2015) Bench-to-bedside development of agonists and antagonists of luteinizing hormone-releasing hormone for treatment of advanced prostate cancer. *Urol Oncol* **33**, 270–274.
40. Rivier C, Rivier J and Vale W (1980) Antireproductive effects of a potent gonadotropin-releasing hormone antagonist in the male rat. *Science* **210**, 93–95.
41. Russell L (1977) Movement of spermatocytes from the basal to the adluminal compartment of the rat testis. *Am J Anat* **148**, 313–328.
42. Russell L (1977) Observations on rat Sertoli ectoplasmic ('junctional') specializations in their association with germ cells of the rat testis. *Tissue Cell* **9**, 475–498.
43. Russell L and Clermont Y (1976) Anchoring device between Sertoli cells and late spermatids in rat seminiferous tubules. *Anat Rec* **185**, 259–278.
44. Russell LD and Griswold MD, eds. (1993) *The Sertoli Cell*. Cache River Press, Clearwater, FL.
45. Ruwanpura SM, McLachlan RI and Meachem SJ (2010) Hormonal regulation of male germ cell development. *J Endocrinol* **205**, 117–131.
46. Schwach G, Oudry N, Giliberto JP, Broqua P, Luck M, Lindner H and Gurny R (2004) Biodegradable PLGA microparticles for sustained release of a new GnRH antagonist: part II. In vivo performance. *Eur J Pharm Biopharm* **57**, 441–446.
47. Show MD, Anway MD, Folmer JS and Zirkin BR (2003) Reduced intratesticular testosterone concentration alters the polymerization state of the Sertoli cell intermediate filament cytoskeleton by degradation of vimentin. *Endocrinology* **144**, 5530–5536.
48. Shupe J, Cheng J, Puri P, Kostereva N and Walker WH (2011) Regulation of Sertoli-germ cell adhesion and sperm release by FSH and nonclassical testosterone signaling. *Mol Endocrinol* **25**, 238–252.
49. Sinha Hikim AP, Lue Y, Diaz-Romero M, Yen PH, Wang C and Swerdloff RS (2003) Deciphering the pathways of germ cell apoptosis in the testis. *J Steroid Biochem Mol Biol* **85**, 175–182.
50. Sinha Hikim AP, Rajavashisth TB, Sinha Hikim I, Lue Y, Bonavera JJ, Leung A, Wang C and Swerdloff RS (1997) Significance of apoptosis in the temporal and stage-specific loss of germ cells in the adult rat after gonadotropin deprivation. *Biol Reprod* **57**, 1193–1201.
51. Sinha Hikim AP and Swerdloff RS (1993) Temporal and stage-specific changes in spermatogenesis of rat after gonadotropin deprivation by a potent gonadotropin-releasing hormone antagonist treatment. *Endocrinology* **133**, 2161–2170.
52. Tang EI, Lee WM and Cheng CY (2016) Coordination of actin- and microtubule-based cytoskeletons supports transport of spermatids and residual bodies/phagosomes during spermatogenesis in the rat testis. *Endocrinology* **157**, 1644–1659.
53. Tone S, Sugimoto K, Tanda K, Suda T, Uehira K, Kanouchi H, Samejima K, Minatogawa Y and Earnshaw WC (2007) Three distinct stages of apoptotic nuclear condensation revealed by time-lapse imaging, biochemical and electron microscopy analysis of cell-free apoptosis. *Exp Cell Res* **313**, 3635–3644.
54. Upadhyay RD, Kumar AV, Ganeshan M and Balasinor NH (2012) Tubulobulbar complex: cytoskeletal remodeling to release spermatozoa. *Reprod Biol Endocrinol* **10**, 27.
55. Ushiki T and Ide C (1988) A modified KOH-collagenase method applied to scanning electron microscopic observations of peripheral nerves. *Arch Histol Cytol* **51**, 223–232.
56. van Kroonenburgh MJ, Beck JL, Vemer HM, Rolland R, Thomas CM and Herman CJ (1986) Effects of a single injection of a new depot formulation of an LH-releasing hormone agonist on spermatogenesis in adult rats. *J Endocrinol* **111**, 449–454.
57. Vidal JD and Whitney KM (2014) Morphologic manifestations of testicular and epididymal toxicity. *Spermatogenesis* **4**, e979099.
58. Walker WH (2011) Testosterone signaling and the regulation of spermatogenesis. *Spermatogenesis* **1**, 116–120.
59. Walker WH and Cheng J (2005) FSH and testosterone signaling in Sertoli cells. *Reproduction* **130**, 15–28.
60. Wang F, Zhang Q, Cao J, Huang Q and Zhu X (2008) The microtubule plus end-binding protein EB1 is involved in Sertoli cell plasticity in testicular seminiferous tubules. *Exp Cell Res* **314**, 213–226.
61. Ward JA, Furr BJ, Valcaccia B, Curry B, Bardin CW, Gunsalus GL and Morris ID (1989) Prolonged suppression of rat testis function by a depot formulation of Zoladex, a GnRH agonist. *J Androl* **10**, 478–486.
62. Weinbauer GF, Respondek M, Themann H and Nieschlag E (1987) Reversibility of long-term effects of GnRH agonist administration on testicular histology and sperm production in the nonhuman primate. *J Androl* **8**, 319–329.
63. Wong CH, Xia W, Lee NP, Mruk DD, Lee WM and Cheng CY (2005) Regulation of ectoplasmic specialization dynamics in the seminiferous epithelium by focal adhesion-associated proteins in testosterone-suppressed rat testes. *Endocrinology* **146**, 1192–1204.
64. Xiao X, Mruk DD, Wong CK and Cheng CY (2014) Germ cell transport across the seminiferous epithelium during spermatogenesis. *Physiology (Bethesda)* **29**, 286–298.
65. Yan HH, Mruk DD, Lee WM and Cheng CY (2007) Ectoplasmic specialization: a friend or a foe of spermatogenesis? *Bioessays* **29**, 36–48.